Defect-mode-like transmission induced by weak nonlinearity in one-dimensional perfect photonic crystals

Daoud Mansour and Khaled Senouci*

University of Mostaganem Abdelhamid Ibn Badis, Laboratoire de Structure, Elaboration et Application des Matériaux Moléculaires (SEA2M), B.P. 227, 27000, Mostaganem, Algeria

(Received 30 August 2019; accepted 26 February 2020; published 22 April 2020)

We investigate numerically the effect of weak Kerr nonlinearity on the transmission spectrum of a one-dimensional (1D) δ-function photonic crystal. A new and interesting phenomenon is observed. It is found that, for weak defocusing nonlinearity, a defect-mode-like (DML) resonance peak is obtained inside the photonic band gap (PBG). That means that a weak nonlinearity acts as a defect introduced in a 1D perfect photonic crystal. A total transmission of this peak is found for a critical value of nonlinearity strength $|\alpha_c|$, while above this value a splitting of the DML resonance peak is observed. Calculations of the spatial dependence of the electric-field intensity reveal that DML resonance peaks have a similar origin as the well-known gap solitons appearing in nonlinear systems. The influences of nonlinearity strength, refractive index, incident angle, number of periods, and polarization on this DML resonance peak are analyzed.

DOI: 10.1103/PhysRevA.101.043830

I. INTRODUCTION

Wave propagation in periodic photonic crystals (PCs) has been intensively studied in the last three decades both theoretically and experimentally [1–6]. PCs are periodic structures of dielectric materials with alternating regions of high and low dielectric constants. The main features of PCs are the presence of forbidden- and allowed-frequency regions called photonic band gaps (PBGs). The formation of photonic band gaps in conventional PCs originates from Bragg scattering, which is strongly dependent on the incidence angle, lattice constant, and polarization. It is possible to have a localized defect mode or state of photons at a particular frequency inside the photonic band gap by introducing an appropriate defect layer into the PC or by removing a single layer from the structure [7–10]. This is the consequence of the breaking of the spatial periodicity of the structure. This localized defect state is caused by multiple scattering and interference. It was found that this defect mode can be tuned easily to any frequencies inside the photonic band gap by changing the thickness, location, and refractive index of the defect layer [11–14]. One-dimensional (1D) PCs with defects can be used as filters and splitters since the defect modes lead to the selective transmission [15–17]. PCs have been applied in many areas, especially in optical devices such as filters, waveguides, diode lasers, photon polarization spectroscopy, etc. [18–23]. 1D PCs are usually used for their simplicity as reference models in order to understand the band diagram and the transmission spectrum, showing the PBG. They can easily be realized by modern experimental methods through simple deposition methods in comparison with two- and three-dimensional (2D and 3D) PCs.

On the other hand, the presence of nonlinearity is known to lead to a much richer and more complex optical response to light. Interesting phenomena are observed when nonlinear material response to light intensity is taken into account. The Kerr effect [24], nonlinear resonances [25,26], divergences, chaos [27], self-trapping and dynamical localization [28] have been revealed by the study of nonlinearity in periodic structures. It was also found that nonlinearity gives rise to light localization in periodic photonic lattices [29]. Other nonlinear effects, such as optical switching [30] and optical bistability [31], have been studied and observed experimentally. The existence of the so-called gap solitons, as a consequence of nonlinear wave interaction, discovered by Chen and Mills [32] in one-dimensional (1D) superlattices was studied both analytically and numerically in one-dimensional photonic crystals [33,34]. Such gap solitons have been experimentally observed in fiber Bragg gratings [35,36] and in AlGaAs waveguides [37,38].

The optical Kerr effect related to the change in refractive index of the medium which is directly induced by the electric field of incident light leads to self-focusing [39] or self-defocusing [40]. The magnitude of refractive-index change is proportional to the square of light electric-field strength E or the light intensity I, i.e., $n = n_0 + n_2|E|^2$ or $n = n_0 + n_2 I$, where n_0 represents the linear refractive index of the medium, and n_2 is the characteristic nonlinear coefficient of the material. The nonlinearity of the PC is important when designing nonlinear devices such as optical diodes [41–43], switches, and limiters [42–44] that operate on the basis of the optical Kerr effect.

The purpose of this paper is to investigate numerically the effect of a weak defocusing Kerr nonlinearity on the transmission properties of one-dimensional (1D) δ-function periodic photonic crystals. A very important and interesting phenomenon is observed when a very weak defocusing

*Corresponding author: khaled.senouci@univ-mosta.dz

nonlinearity is applied to a 1D perfect photonic crystal. Here we demonstrate numerically nonlinearity-induced defect-mode-like transmission in a 1D PC without defects. A resonance peak of the transmission appears in the center of the photonic band gap (PBG). The influence of nonlinearity strength, angle of incidence, number of periods of the photonic crystal, and polarization on this defect mode-like transmission has also been investigated.

Note that this investigation is different from that of Markos and Soukoulis [45] since we examine the effect of a weak defocusing nonlinearity on light transmission. We focus our study on the role played by the nonlinearity strength and refractive index for the formation and splitting of localized modes within the photonic band gap, while they studied the phenomenon of optical bistability in nonlinear structures.

II. MODEL DESCRIPTION

To investigate the effect of nonlinearity on the wave propagation in a one-dimensional photonic crystal, we consider a one-dimensional Kronig-Penney model with $N\delta$-function layers distributed periodically at $x = na$, $n = 0, 1 \ldots, N-1$. Here, a is the lattice constant. Such a periodic medium represents the simplest model for a one-dimensional PC.

The electromagnetic waves outside the nonlinear structure are described by [45]

$$E(x) = \begin{cases} E_i e^{-ikx} + E_r e^{ikx}, & x \geqslant Na \\ E_t e^{-ikx}, & x \leqslant 0. \end{cases} \tag{1}$$

Here we considered an incident plane wave $E_i e^{-ikx}$ with wave number k, from the right which gives rise to a reflected wave, $E_r e^{ikx}$, as well as a transmitted wave $E_t e^{-ikx}$ where the wave vector $k = w/c$, w is the optical frequency, and c is the vacuum speed of light.

Inside the structure, the electric field for the transverse-electric (TE) mode satisfies the time-independent wave equation [45,46]

$$\frac{d^2E(x)}{dx^2} + \beta \sum_{n=1}^{N} [1 + \alpha |E(x)|^2)] E(x)\delta(x - na) = 0. \tag{2}$$

Here $E(x)$ is the electric field at the x axis. $\beta = \frac{\varepsilon w^2}{c^2}$ where ε is the electric permittivity. For simplicity the lattice spacing is taken to be unity throughout this work ($a = 1$). Equation (2) is formally equivalent to the Kronig-Penney model of electrons [46–49]. From the computational point of view it is more useful to consider the discrete version of this equation, which is called the generalized Poincaré map and can be derived without any approximation from equation (2). It reads [45]

$$E_{n+1} = [2\cos k - \beta(1 + \alpha |E(x)|^2) k \sin k] E_n - E_{n-1}, \tag{3}$$

where E_n is the value of the electric-field amplitude in TE polarization at site n. This representation relates the values of the electric-field amplitudes at three successive discrete locations along the x axis. The solution of the above equation is carried out iteratively by taking for our initial conditions the following values at sites 0 and 1: $E_0 = 1$ and $E_1 = \exp(-ik)$. We consider here an electromagnetic wave having a wave vector k incident at site N from the right. The transmission coefficient T can then be expressed as [45]

$$T = \frac{4\sin^2(k)|E_0|^2}{\left|e^{-ik}E_n - E_{n-1}\right|^2}. \tag{4}$$

Thus T depends only on the values of the electric-field amplitude at the end sites, E_{n-1}, E_n, which are evaluated from the iterative equation (3).

III. RESULTS AND DISCUSSION

We perform numerical calculations on Kerr nonlinearity effects on the transmission properties of a one-dimensional perfect photonic crystal. The main result of the present work concerns only the weak defocusing nonlinearity regime $\alpha < 0$. In the presence of a Kerr nonlinearity, the refractive index of structure is affected by the electromagnetic-field intensity, leading to a modification in the transmission characteristic of a one-dimensional photonic band structure. We investigate the effect of weak negative (defocusing) nonlinearity on the transmission spectrum. Here we observe numerically nonlinearity-induced defect-mode-like transmission in 1D perfect PC. The dependence of the defect mode-like transmission on the nonlinearity strength, the index of refraction, the structure length (the number of periods) and the angle of incidence is also studied. We investigate the case of both transverse electric (TE) and transverse magnetic (TM) polarizations. The transmission spectrum of this structure can be calculated by using the transfer-matrix method.

A. Effect of nonlinearity strength

To highlight the effect of a nonlinear interaction, we first discuss only the TE polarization of propagating electromagnetic waves at normal incidence. We choose the number of the structure periods to be 44. The refractive index of these layers is assumed to be $n = 3.5$, which is the value for silicon. Figure 1 shows the transmission spectrum of the 1D perfect photonic crystal for linear and nonlinear cases. For the linear case ($\alpha = 0$), one can see clearly that there is a photonic band gap (PBG) in the range from 0.349 to 0.391 μm, as shown in Fig. 1(a). When a very weak defocusing nonlinearity $\alpha = -10^{-6}$ is applied, a single transmission peak is produced at $\lambda_0 = 0.3728$ μm within the same PBG as shown in Fig. 1(b). This transmission peak is referred to as a defect-mode-like (DML) transmission peak. This means that a weak defocusing nonlinearity acts as a defect introduced into a 1D perfect photonic crystal. This result is of a great practical importance since we can have a defect-mode-like transmission without introducing a defect in a perfect photonic crystal by choosing an appropriate nonlinear material. To see the effect of nonlinearity on this defect-mode-like transmission peak, we calculated the transmission spectra for different nonlinearity strengths. The results are displayed in Fig. 2(a). We can observe that the defect-mode-like peak starts to appear for $|\alpha| = 10^{-7}$ and its amplitude increases as we increase the nonlinearity in magnitude and reaches its maximum value (total transmission) for a critical nonlinearity strength $|\alpha_c| = 1.2 \times 10^{-7}$ (as shown in the inset) while its position is not affected. We note that $|\alpha_c|$ depends on the nature of the material (the refractive index n).

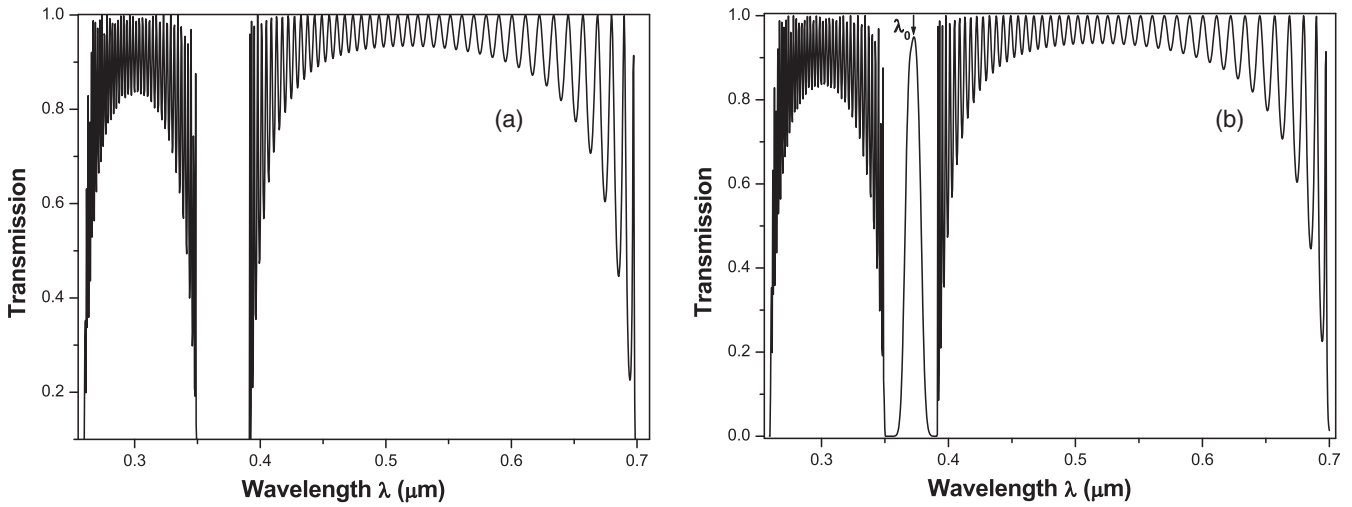

FIG. 1. Transmission spectra as a function of the wavelength for a structure of 44 layers and a refractive index $n = 3.5$ for (a) $\alpha = 0$ (linear case). (b) $\alpha = -10^{-6}$ (showing defect-mode-like peak in the PBG).

It was found that nonlinearities change the refraction index since $n = n_0 + n_2|E|^2$ (n_0 being the linear refraction index, n_2 being the Kerr nonlinearity coefficient, and E being the electric-field amplitude) leading to a shift of defect modes and PBG in a defect-containing 1D photonic crystal to lower or higher wavelengths depending on the sign of the Kerr nonlinearity n_2 [24,50]. It is important to note that, in our case, the PBG and the position of the defect-mode-like peak remain unchanged since the nonlinearity is very weak.

Figure 2(b) displays the transmission spectra for $|\alpha| > |\alpha_c|$. This figure shows that, beyond $|\alpha_c|$, a splitting of the defect-mode-like peak begins to appear by presenting two bumps that separate by increasing $|\alpha_c|$ and forming two distinct peaks of the same intensity as the nonlinearity strength is increased (see red-solid curve).

Insight into the physical origin of the DML transmission peak can be obtained by plotting the spatial dependence of the electric-field intensity. Figure 3 shows the variation of the field intensity $|E|^2$ as a function of the distance at wavelength $\lambda_0 = 0.3728$ μm corresponding to transmission peak of Fig. 1(b) (indicated by an arrow) for which $T = 1$. Figure 3 shows that the envelope of $|E|^2$ seems to be similar to that of a sine-Gordon soliton and is fit accurately by the function $f(x) = A\cosh^{-2}[\gamma(x - x_0)]$, where A is the maximum value of E, γ is a fitting parameter, and $x_0 = 22.5$ is the mean distance. We can than conclude that the DML peak has a similar origin as the well-known gap solitons appearing in nonlinear systems with a spatial periodicity.

To understand the properties of the DML peak splitting for $|\alpha| = 500 \times 10^{-7}$, We have carried out calculations of the electric field intensity at wavelengths $\lambda_L = 0.3581$ μm and $\lambda_R = 0.3874$ μm corresponding to the two peaks observed in Fig. 2(b) (red-solid curve). We can clearly see from Fig. 3 that $|E|^2$ has the same gap soliton profile for the two peaks. However, the field amplitude for the left peak is greater than that of the right peak.

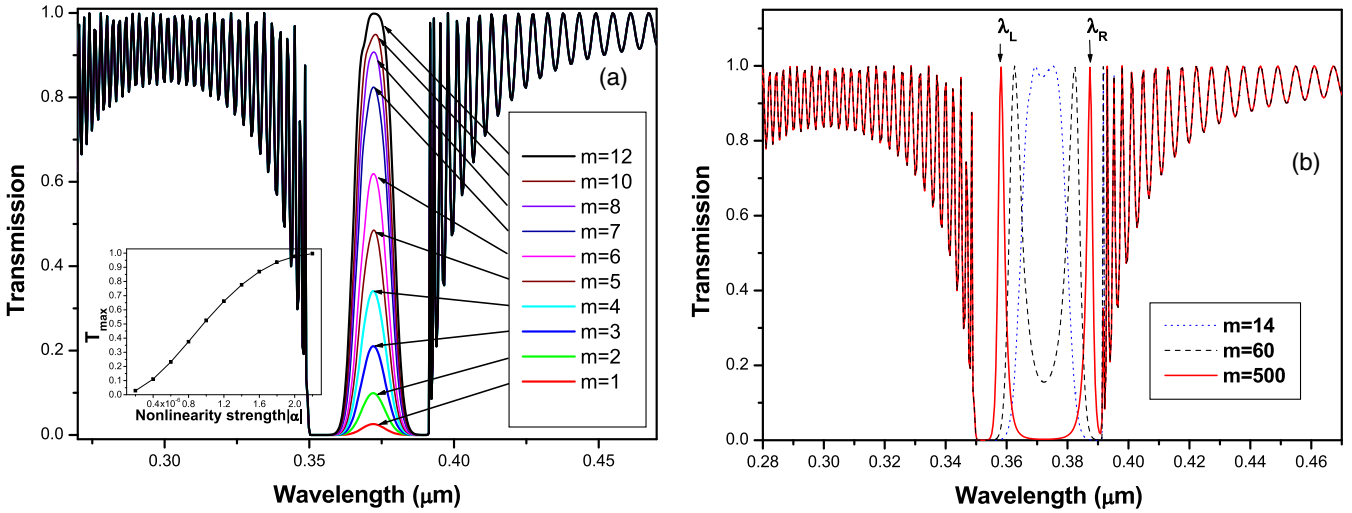

FIG. 2. (a) Transmission spectra as a function of the wavelength for a structure of 44 layers and a refractive index $n = 3.5$ and different nonlinearity strengths $|\alpha| = m \times 10^{-7}$ with $m = 1$ to 12. Inset shows maximum of transmission as a function of nonlinearity strength $|\alpha|$. (b) Transmission spectra as a function of wavelength for $|\alpha| > |\alpha_c|$ with $m = 14$, 60, and 500.

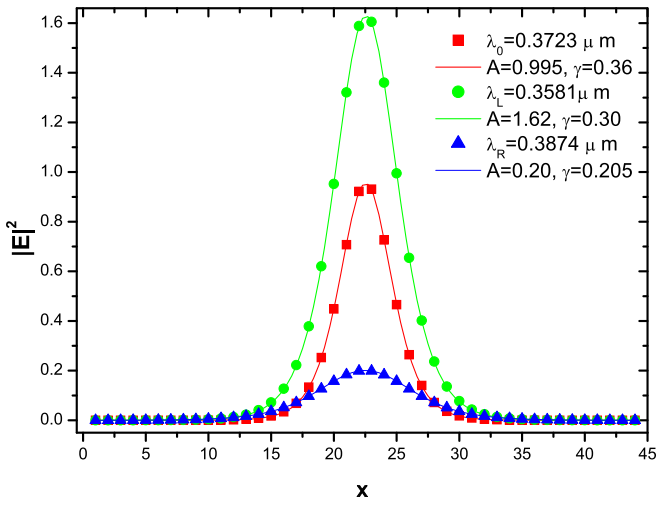

FIG. 3. Spatial dependence of normalized field intensity $|E|^2/10^7$ at wavelength corresponding to DML peak: $\lambda_0 = 0.3728$ μm corresponds to the single transmission peak for $|\alpha| = 1.2 \times 10^{-7}$ [indicated by an arrow in Fig. 1(b)], $\lambda_L = 0.3581$ μm and $\lambda_R = 0.3874$ μm (where λ_L and λ_R correspond to right peak and left peak wavelengths, respectively) for $|\alpha| = 500 \times 10^{-7}$ [showed by arrows in Fig. 2(b)]. Solid curves correspond to sine-Gordon function fit: $f(x) = A\cosh^{-2}[\gamma(x - x_0)]$. A represents the field amplitude, γ is a fitting parameter and $x_0 = 22.5$. The values of A and γ for each wavelength are shown in the figure.

To check the effect of nonlinearity strength on DML splitting, we calculated the transmission spectrum for different values of nonlinearity strength $|\alpha| = m \times 10^{-7}$with m=200, 300, 400, 500, and 700.The results are displayed in Fig. 4. We observe that, when the nonlinearity strength increases, the DML splitting continues to occur but the number of peaks remains the same, i.e., two peaks in the regime of weak nonlinearity strength. We can also observe that these peaks separate far away from each other as the nonlinearity strength is increased. We calculated the wavelength difference $\Delta\lambda$ between two peaks represented by $\Delta\lambda = \lambda_R - \lambda_L$ [where λ_R and λ_L correspond to right peak and left peak wavelengths, respectively, as indicated in Fig. 2(b)], for different values of nonlinearity strength. The results reveal that the wavelength difference $\Delta\lambda$ between the peaks increases logarithmically with the nonlinearity strength (see inset of Fig. 4).

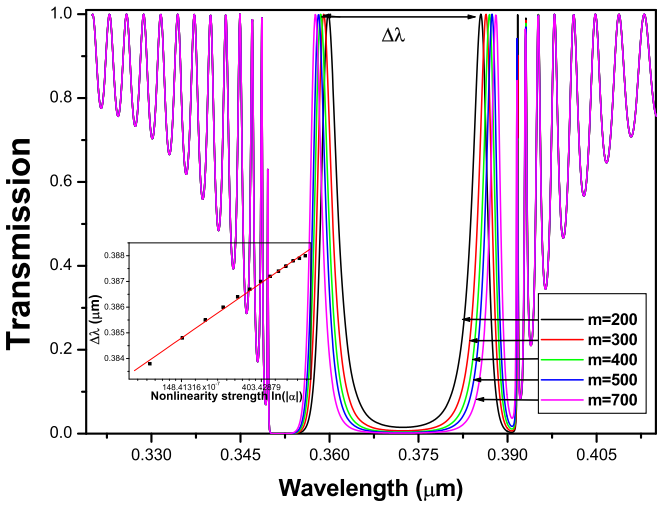

FIG. 4. Transmission spectra as a function of the wavelength for a structure of 44 layers and a refractive index $n = 3, 5$ and different nonlinearity strengths $|\alpha| = m \times 10^{-7}$ with $m = 200$ to 700. Inset shows calculated wavelength difference $\Delta\lambda = \lambda_R - \lambda_L$ between two peaks as a function of nonlinearity strength $\ln(|\alpha|)$. Arrows are used for the printed version.

B. Effect of index of refraction

To investigate the refractive-index effect on the defect mode-like peak, we calculate the transmission spectrum for a fixed nonlinearity strength $|\alpha| = 10^{-6}$ and a structure of 44 layers for a range of refractive index n [3.20 to 3.80]. The values of the index of refraction are chosen according to some optical materials [51]. The results are displayed in Fig. 5. We observe that a transmission peak (defect mode-like resonance) inside the photonic band gap starts to appear for $n = 3.2$. Its intensity increases with increasing n [see Figs. 5(a), 5(b) and also 6]. Thus, the higher refractive index leads to higher resonance peak and thus is more suitable for the design of filtering devices. For $n = 3.80$, a splitting of the defect mode-like peak is observed, as shown in Fig. 5(c). A dual defect mode-like with unequal peak height clearly located inside the PBG is obtained. The position of these peaks and the PBG are slightly shifted to higher wavelengths as we increase the refractive index, as shown in the inset of Fig. 6.

As we discussed in the previous section, the total transmission of the defect mode-like peak depends on a critical nonlinearity strength $|\alpha_c|$, which itself depends on the refractive index n. For each value of refraction index n, we calculated the transmission spectra for different nonlinearity strengths and estimated the critical nonlinearity strength $|\alpha_c|$ (for different values of n). The results are displayed in Fig. 7. It can be seen from this figure that $|\alpha_c|$ decreases exponentially with refractive index n as $|\alpha_c| = A\exp(-n/B)$, with $A = 15.2353 \times 10^4$ and $B = 0.1379$.

To evaluate the behavior of the wavelength difference between the two peaks, we plot the transmission spectra for different values of refractive index $n = 3.80$, 3.82, and 3.84. The results are displayed in Fig. 8. This figure shows that as the refractive index n increases, the peak positions shift to longer wavelengths. It is also observed that the two peaks persist to appear but the magnitude of the first peak (left peak) decreases by increasing n while that of the second peak (right peak) remains unchanged. The calculated wavelength difference $\Delta\lambda$ between the two peaks increases linearly with refractive index n (see inset of Fig. 8).

C. Effect of the incidence angle and polarization

To investigate the effect of the angle of incidence of the electromagnetic wave on the defect-mode-like peak, we calculate the transmission spectrum for a fixed nonlinearity strength $|\alpha| = 1.2 \times 10^{-6}$ corresponding to a maximum resonance (total transmission), a structure of 44 layers and a refractive

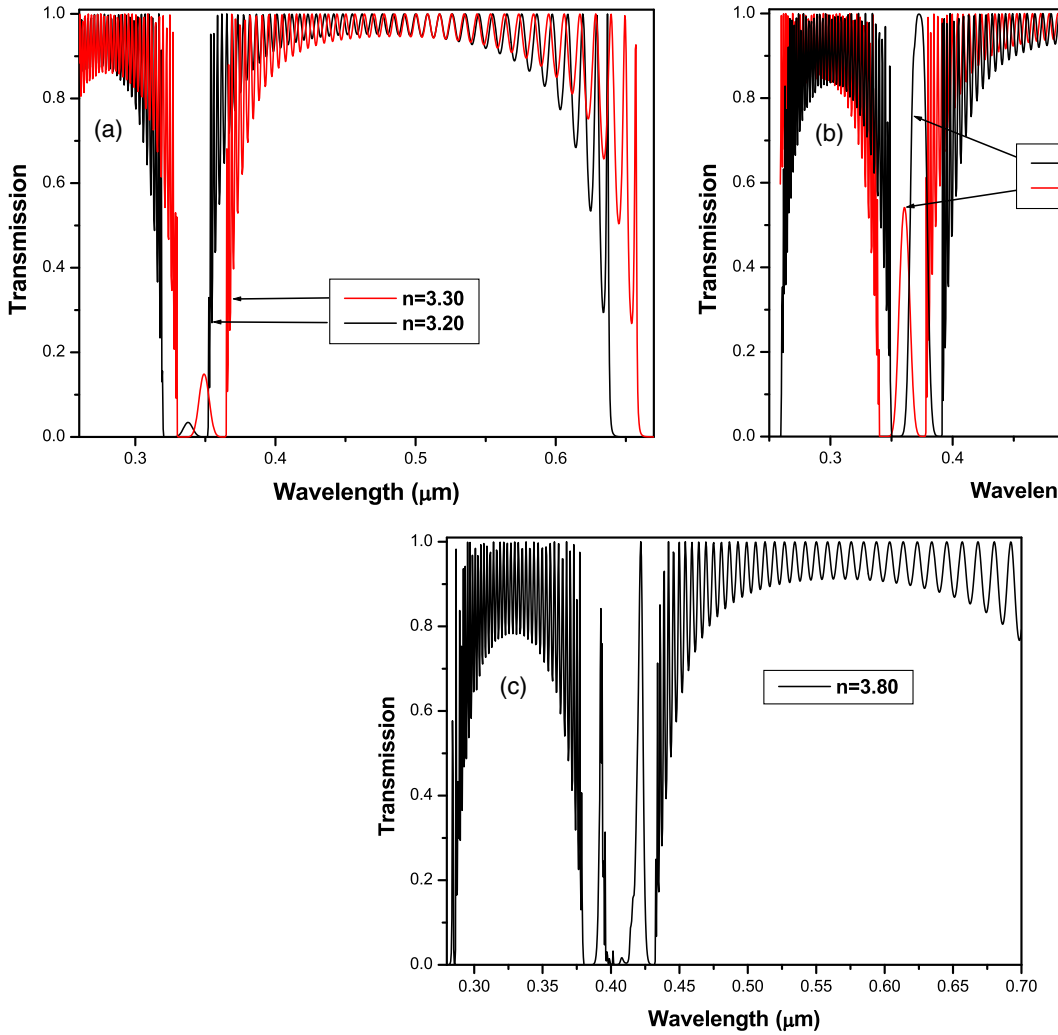

FIG. 5. Effect of the refractive index n on the defect-mode-like peak. Transmission spectrum for a structure of 44 layers and $\alpha = -1.2 \times 10^{-6}$ for different refraction indices (a) $n = 3.2$ and $n = 3.3$, (b) $n = 3.4$ and $n = 3.5$, and (c) $n = 3.80$. A dual defect-mode-like peak with unequal peak height clearly observed inside the PBG is obtained for $n = 3.80$. Arrows are used for the printed version.

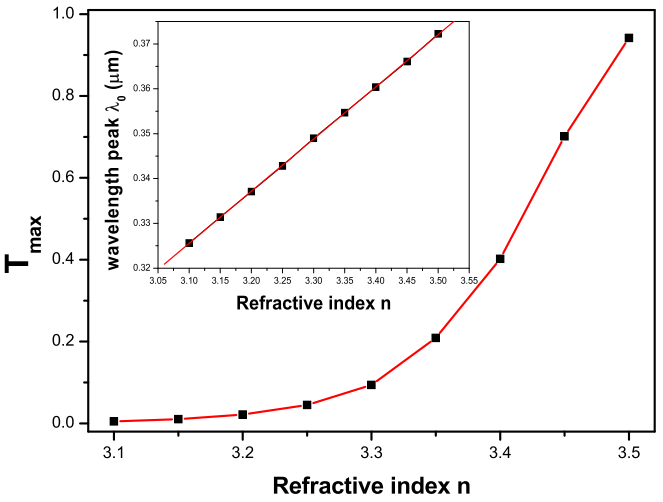

FIG. 6. Maximum of the transmission as a function of the refractive index n. Inset shows calculated wavelength peak λ_0 as a function of the refractive index n for a structure of 44 layers for a defocusing nonlinearity, $\alpha = -10^{-6}$. Solid line corresponds to a linear fit.

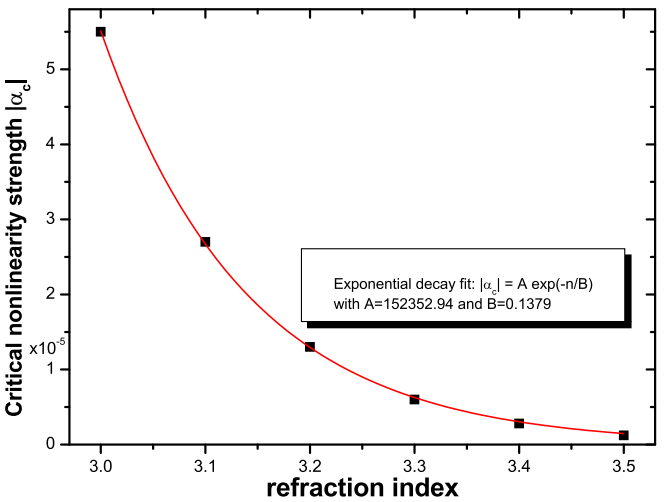

FIG. 7. Critical nonlinearity strength $|\alpha_c|$ for total transmission as a function of refractive index n for a structure of 44 layers at normal incidence. Solid curve corresponds to an exponential-decay fit: $|\alpha_c| = A \exp(-n/B)$, with $A = 15.2353 \times 10^4$ and $B = 0.1379$.

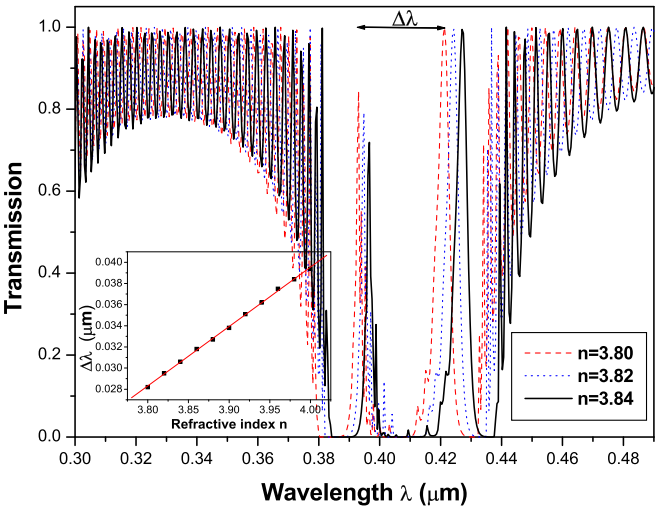

FIG. 8. Transmission spectra as a function of the wavelength for a structure of 44 layers and different refractive indexes $n = 3.80$, $n = 3.82$, and $n = 3.84$ for $|\alpha| = 10^{-6}$. Inset shows calculated wavelength difference $\Delta\lambda = \lambda_R - \lambda_L$ as a function of refractive index n.

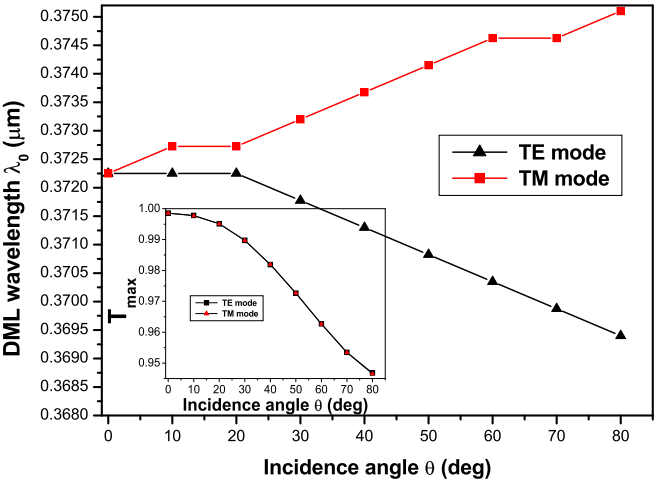

FIG. 10. Defect-mode-like wavelength λ_0 as a function of the incidence angle θ. Inset shows maximum of the transmission of the defect-mode-like peak as a function of angle of incidence for a structure of 44 layers and a refractive index of 3.5 and $|\alpha| = 10^{-6}$.

index $n = 3.5$. In Fig. 9, both TE and TM mode transmission spectra are plotted at distinct angles of incidence, $\theta = 0^\circ$, $\theta = 5^\circ$, and $\theta = 10^\circ$, respectively. This figure shows how the defect-mode-like peak can be affected by the incident angle. It is very clear from this figure that the amplitude of the defect-mode-like peak decreases with increasing angle of incidence for both TE and TM polarization. It is also observed that its peak wavelength (position) gradually shifts with photonic band gap in the direction of lower wavelength upon increasing the incident angle for TE polarization [Fig. 9(a)] while for the TM mode it shifts to higher wavelengths [Fig. 9(b)]. The dependence of the defect-mode-like wavelength and its intensity on the angle of incidence for both TE and TM polarizations is further illustrated in Fig. 10. It is clear from this figure that both the intensity and the position of the defect-mode-like peak are affected by the angle of incidence. The DML peak intensity decreases as the angle of incidence increases and seems to be very insensitive to the light polarization (see inset of Fig. 10). The resonance wavelength of the DML peak gradually shifts in the direction of shorter wavelengths for the TE mode while it gradually shifts in the direction of longer wavelengths for the TM mode (Fig. 10). Beyond $\theta = 20^\circ$, it seems to linearly increase with angle of incidence for the TM mode or linearly decrease with angle of incidence for TE-polarized light.

D. Effect of number of periods

To further study the effect of the number of layers of the photonic crystal on the defect-mode-like peak, we numerically calculate the transmission spectra for a fixed nonlinearity strength $|\alpha| = 10^{-6}$ and a refractive index $n = 3.5$ for different values of the number of periods $N = 36$, 40, 44, and

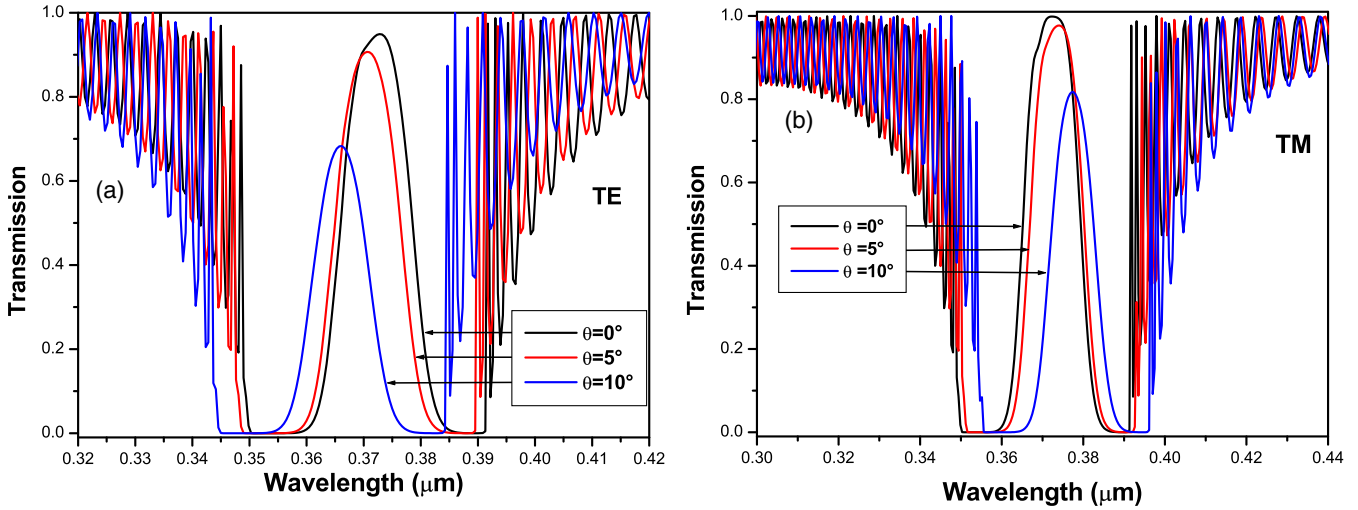

FIG. 9. Effect of the incidence angle on the defect-mode-like peak. Transmission spectrum for a structure of 44 layers, $|\alpha| = 1.2 \times 10^{-6}$ and $n = 3.5$ at distinct angles of incidence, $\theta = 0^\circ$, $\theta = 5^\circ$, and $\theta = 10^\circ$ for (a) TE mode and (b) TM mode. Arrows are for the printed version.

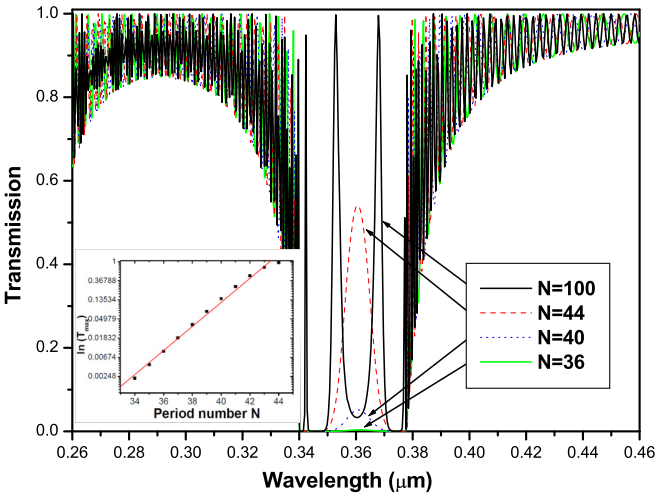

FIG. 11. Transmission spectra at normal incidence for $n = 3.4$, $|\alpha| = 1.2 \times 10^{-6}$, and different number of periods $N = 36$, 40, 44, and 100. Inset shows defect-mode-like peak intensity (logarithmic scale) versus the number of periods N. Arrows are for the printed version.

100. We choose $\theta = 0^\circ$ since we found a maximum-amplitude DML peak at normal incidence. The results are displayed in Fig. 11. One can see that a single defect-mode-like peak appears inside the PBG for $N = 36$. From this figure it is evident that, as the number of periods N increases, resonance becomes stronger. As we increase the number of periods from $N = 34$ to $N = 44$, the peak amplitude of the defect-mode-like peak increases, as shown in the inset. The maximum of transmission (peak intensity) seems to increase exponentially with the number of layers. For $N = 100$, a splitting of this defect-mode-like peak is observed with a total transmission (black solid curve in Fig. 11). A dual defect-mode-like peak with equal peak heights clearly appears inside the PBG. This interesting result is of great practical importance since it can be used as a narrowband transmission filter. A dual-channel filter can be obtained by increasing the number of periods in the nonlinear photonic structure.

IV. CONCLUSION

In conclusion, we have studied in this paper the effect of a weak defocusing Kerr nonlinearity on the transmission properties of one-dimensional (1D) photonic crystals (PCs) with no defects. A very important and interesting phenomenon is observed when a very weak defocusing nonlinearity is applied to a 1D zero-defect photonic crystal. We found the presence of a defect-mode-like peak (i.e., a single resonance transmission peak) within the photonic band gap with a total transmission. This means that a weak negative nonlinearity acts as a defect introduced in a perfect 1D photonic crystal. This is a very interesting result. We can choose an appropriate nonlinear material to have a defect-mode-like peak without introducing a defect into a photonic crystal. With the presence of this resonant peak in transmission, the structure can be used as a narrowband transmission filter. We demonstrate numerically that the intensity of the defect-mode-like peak depends on the nonlinearity strength, the refractive index, and number of layers whereas its position depends only on the angle of incidence and the refractive index.

We also found that the peak wavelength of the defect mode-like shifts toward short wavelengths as the angle of incidence increases for TE mode while it shifts towards long wavelengths for the TM mode. A total transmission of the DML peak is observed for a critical nonlinearity strength $|\alpha_c|$ which itself depends on the refractive index n. We found that $|\alpha_c|$ decreases exponentially with refractive index n. We also found a critical refractive index n_c and a critical period number of the photonic structure N_c above which a splitting of the defect-mode-like peak is observed. The splitting of the defect-mode-like peak is also observed for $|\alpha| > |\alpha_c|$. Consequently, by increasing the period number N of the PC or the refractive index n, a dual defect-mode-like peak is obtained, leading to a possible design of a narrow-band transmission multichannel tunable filter. We also found that the wavelength difference $\Delta\lambda$ between the two peaks increases logarithmically with the nonlinearity strength whereas it increases linearly with refractive index.

It is important to note that this DML phenomenon is not observed if we consider a focusing nonlinearity ($\alpha > 0$). It is interesting to study the properties of the splitting of the defect-mode-like peak as a function of different parameters. Also, the DML transmission peak can be tuned physically by using external agents such as an external electric field, magnetic field, or temperature. In our case, it is easy to control the defect-mode-like peak by applying a bias voltage (an external electric field) to the 1D photonic crystal. It is thus interesting to study the splitting properties of the DML in the presence of an external electric field. We have studied the response of a nonlinear δ-function layer and it is important to extend this study to a nonlinear finite-width layer. All these effects should be the subject of a forthcoming presentation.

ACKNOWLEDGMENTS

One of the authors (K.S.) would like to acknowledge the International Centre for Theoretical Physics (ICTP, Trieste, Italy) for its hospitality where part of this work was done. The author also gratefully acknowledges support from the physics department of the University of Mostaganem (Algeria). This work has been supported by "Projet de Recherche Formation Universitaire" PRFU (Grant No. B00L02UN270120180001), approved in 2018.

[1] E. Yablonovitch, Phys. Rev. Lett. **58**, 2059 (1987).
[2] S. John, Phys. Rev. Lett. **58**, 2486 (1987).
[3] G. Antonopoulos, F. Benabid, T. A. Birks, D. M. Bird, J. C. Knight, and P. St. J. Russell, Opt. Express **14**, 3000 (2006).
[4] Y. Yang, Y. F. Xu, T. Xu, H.-X. Wang, J.-H. Jiang, X. Hu, and Z. H. Hang, Phys. Rev. Lett. **120**, 217401 (2018).
[5] S. B. Hasan, A. P. Mosk, W. L. Vos, and A. Lagendijk, Phys. Rev. Lett. **120**, 237402 (2018).

[6] J. D. Joannopoulos, S. G. Johnson, J. N. Winn, and R. D. Meada, *Photonic Crystals: Modeling the Flow of Light* (Princeton University Press, Princeton, 2008).

[7] Z. M. Jiang, B. Shi, D. T. Zhao, J. Liu, and X. Wang, Appl. Phys. Lett. **79**, 3395 (2001).

[8] M. Scalora, J. P. Dowling, C. M. Bowden, and M. J. Bloemer, Phys. Rev. Lett. **73**, 1368 (1994).

[9] K.- Y. Xu, X. Zheng, C.-L. Li, and W. L. She, Phys. Rev. E **71**, 066604 (2005).

[10] C.-J. Wu and Z. H. Wang, Prog. Electromagn. Res. **103**, 169 (2010).

[11] Q. Zhu and Y. Zhang, Optik (Munich, Ger.) **120**, 195 (2009).

[12] S. K. Srivastava, M. Upadhyay, S. K. Awasthi, and S. P. Ojha, Opt. Photonics J. **2**, 230 (2012).

[13] H. Y. Liu, S. Liang, Q.-F. Dai, L.-J. Wu, S. Lan, A. V. Gopal, V. A. Trofimov, and T. M. Lysak, J. Appl. Phys. **110**, 073101 (2011).

[14] G. L. Shang, G. T. Fei and L. D. Zhang, J. Phys. D: Appl. Phys. **48**, 435304 (2015).

[15] A. H. Aly and H. A. Elsayed, Phys. B (Amsterdam, Neth.) **407**, 120 (2012).

[16] X. Xing, W. Wang, S. Li, W. Zheng, D. Zhang, Q. Du, X. Gao, and B.-Y. Zhang, Optik (Munich, Ger.) **127**, 135 (2016).

[17] S. Jena, R. B. Tokas, S. Thakur, and D. V. Udupa, Phys. E **114**, 113627 (2019).

[18] X. Gu, X. F. Chen, Y. P. Chen, X. L. Zheng Y. X. Xia, and Y. L. Chen, Opt. Commun. **237**, 53 (2004).

[19] F. Ghasemi, S. R. Entezar, and S. Razi, Phys. Lett. A **383**, 2551 (2019).

[20] G. J. Schneider and G. H. Watson, Appl. Phys. Lett. **83**, 5350 (2003).

[21] N. Tsurumachi, M. Abe andM. Arakawa, Jpn. J. Appl. Phys. (1962–1981) **38**, 1400 (1999).

[22] J. A. Monsoriu, C. J. Zapata-Rodriguez, E. Silvestre, and W. D. Furlan, Opt. Commun. **252**, 46 (2005).

[23] M. L. N. Chen, L. J. Jiang, and W. E. I. Sha, Phys. Rev. Appl. **10**, 014034 (2018).

[24] B. Liu, A. Yamilov, and H. Cao, Appl. Phys. Lett. **83**, 1092 (2003).

[25] N. Flytzanis, S. Pnevmatikos, and M. Remoissenet, Phys. D **26**, 311 (1987).

[26] U. Langbein, F. Lederer, T. Peschel, U. Trutschel and D. Mihalache, Phys. Rep. **194**, 325 (1990).

[27] D. L. Shepelyansky, Phys. Rev. Lett. **70**, 1787 (1993).

[28] M. L. Lyra and R. P. A. Lima, Phys. Rev. E **85**, 057201 (2012).

[29] D. N. Neshev, A. A. Sukhorukov, W. Królikowski, and Yu. S. Kivshar, J. Nonlinear Opt. Phys. Mater. **16**, 1 (2007).

[30] N. D. Sankey, D. F. Prelewsitz, and T. G. Brown, Appl. Phys. Lett. **60**, 1427 (1992).

[31] C. J. Herbert and M. S. Malcuit, Opt. Lett. **18**, 1783 (1993).

[32] W. Chen and D. L. Mills, Phys. Rev. Lett. **58**, 160 (1987).

[33] T. P. Lobo, L. E. Oliveira, and S. B. Cavalcanti, Superlattices Microstruct. **112**, 442 (2017).

[34] L. Tkeshelashvili, J. Niegemann, S. Pereira, and K. Busch, Photonics Nanostruct. **4**, 75 (2006).

[35] U. Mohideen, R. E. Slusher, V. Mizrani, T. Erdogan, M. Kuwata-Gonokami, P. J. Lemaire, J. E. Sipe, C. M. de Sterke, and N. G. R. Brodorick, Opt. Lett. **20**, 1674 (1995).

[36] B. J. Eggleton, R. E. Slusher, C. M. de Sterke, Peter A. Krug, and J. E. Sipe, Phys. Rev. Lett. **76**, 1627 (1996).

[37] P. Millar, M. De La Rue, T. F. Krauss, J. S. Aitchison, N. G. R. Broderick, and D. J. Richardson, Opt. Lett. **24**, 685 (1999).

[38] J. P. Prineas, C. Ell, E. S. Lee, G. Khitrova, H. M. Gibbs, and S. W. Koch, Phys. Rev. B **61**, 13863 (2000).

[39] Y. Kominis, Phys. Rev. E **73**, 066619 (2006).

[40] Y. Kominis and K. Hizanidis, Opt. Lett. **31**, 2888 (2006).

[41] M. Scalora, J. P. Dowling, C. M. Bowden, and M. J. Bloemer, J. Appl. Phys. **76**, 2023 (1994).

[42] I. S. Fogel, J. M. Bendickson, M. D. Tocci, M. J. Bloemer, M. Scalora, C. M. Bowden, and J. P. Dowling, Pure Appl. Opt. **7**, 393 (1998).

[43] N. S. Zhao, H. Zhou, Q. Guo, W. Hu, X. B. Yang, S. Lan, and X. S. Lin, J. Opt. Soc. Am. B **23**, 2434 (2006).

[44] V. A. Bushuyev and A. D. Pryamikov, Quantum Electron. **33**, 515 (2003).

[45] P. Markos and C. M. Soukoulis, *Wave Propagation, from Electrons to Photonic Crystals and Left-Handed Materials* (Princeton University Press, Princeton, 2008).

[46] E. Lidorikis, K. Busch, Qiming Li, C. T. Chan and C. M. Soukoulis, Phys. D **113**, 346 (1998).

[47] E. Cota, J. V. José, J. Maytorena, and G. Monsivais, Phys. Rev. Lett. **74**, 3302 (1995).

[48] K. Senouci, N. Zekri, H. Bahlouli, and A. K. Sen, J. Phys.: Condens. Matter **11**, 1823 (1999).

[49] K. Senouci and N. Zekri, Phys. Rev. B **62**, 2987 (2000).

[50] J. Zhang, R. Zhang, and Y. Wang, Optik (Munich, Ger.) **126**, 5052 (2015).

[51] M. Wakaki, K. Kudo, and T. Shibuya, *Physical Properties and Data of Optical Materials* (CRC Press, Boca Raton, 2007).